Available online at www.sciencedirect.com
ScienceDirect
Journal of Power Sources 159 (2006) 1488–1493
JOURNAL OF POWER SOURCES
www.elsevier.com/locate/jpowsour

Sulfur dioxide leaching of spent zinc–carbon-battery scrap

J. Avraamides, G. Senanayake *, R. Clegg

A.J. Parker Cooperative Research Centre for Hydrometallurgy, Murdoch University, Perth, WA 6150, Australia

Received 11 October 2005; received in revised form 28 November 2005; accepted 29 November 2005
Available online 19 January 2006

Abstract

Zinc–carbon batteries, which contain around 20% zinc, 35% manganese oxides and 10% steel, are currently disposed after use as land fill or reprocessed to recover metals or oxides. Crushed material is subjected to magnetic separation followed by hydrometallurgical treatment of the non-magnetic material to recover zinc metal and manganese oxides. The leaching with 2 M sulfuric acid in the presence of hydrogen peroxide recovers 93% Zn and 82% Mn at 25 °C. Alkaline leaching with 6 M NaOH recovers 80% zinc. The present study shows that over 90% zinc and manganese can be leached in 20–30 min at 30 °C using 0.1–1.0 M sulfuric acid in the presence of sulfur dioxide. The iron extraction is sensitive to both acid concentration and sulfur dioxide flow rate. The effect of reagent concentration and particle size on the extraction of zinc, manganese and iron are reported. It is shown that the iron and manganese leaching follow a shrinking core kinetic model due to the formation of insoluble metal salts/oxides on the solid surface. This is supported by (i) the decrease in iron and manganese extraction from synthetic Fe(III)–Mn(IV)–Zn(II) oxide mixtures with increase in acid concentration from 1 M to 2 M, and (ii) the low iron dissolution and re-precipitation of dissolved manganese and zinc during prolonged leaching of battery scrap with low sulfur dioxide.

Keywords: Zinc–carbon battery scrap; Leaching; Sulfur dioxide; Shrinking core kinetic model

1. Introduction

Zinc–carbon batteries have a carbon rod cathode in contact with a moist paste of MnO_2, NH_4Cl and $ZnCl_2$ with the acid electrolyte, all contained in a zinc case which acts as the anode. A plastic or paperboard separator and an asphalt seal are usually present. The discharge reaction produces Mn(III) oxide and $Zn(NH_3)_2Cl_2$(s):

$$2MnO_2(s) + 2NH_4Cl(s) + Zn(s) \rightarrow Mn_2O_3(s) + H_2O(l) + Zn(NH_3)_2Cl_2(s) \quad (1)$$

Large quantities of both metallic and ionic zinc and manganese are contained in the batteries and proper landfill disposal or a suitable recovery process [1,2] is required to reduce groundwater contamination. Salgado et al. [3] described the method of elemental analysis of several types of batteries. Table 1 shows the composition of zinc–carbon battery scrap used in the present study provided by the Korea Institute of Geoscience and Mineral Resources (KIGAM) in Daejeon.

The researchers in KIGAM (Dong-Jin Kim, Jae-Chun Lee and Jeong-Soo Sohn, unpublished data) have carried out the leaching of zinc–carbon battery scrap in:

(i) sulfuric acid media (0.25–2 M) at 40–60 °C in the absence of a reducing agent,
(ii) sodium hydroxide media (2–6 M) at 40–80 °C, or
(iii) sulfuric acid media (0.5–4 M) in the presence of hydrogen peroxide (25–60 °C).

The results obtained in sulfuric acid leaching in the absence of a reducing agent showed low percent dissolution of both metals with no significant improvement at high acid concentrations or high temperatures (>60 °C). The researchers at KIGAM have also selectively leached zinc using sodium hydroxide because Zn(II) dissolves as the complex ion $Zn(OH)_4^{2-}$ in alkaline solutions. Again, the zinc extraction by 5 M NaOH at 80 °C reached 88% and there was no further improvement at higher alkali concentrations. The effects of reaction time, reagent concentration and reaction temperature on the leaching rate of the solid

* Corresponding author. Tel.: +61 8 9360 2833; fax: +61 8 9360 6343.
E-mail address: G.Senanayake@murdoch.edu.au (G. Senanayake).

0378-7753/$ – see front matter © 2005 Elsevier B.V. All rights reserved.
doi:10.1016/j.jpowsour.2005.11.081

Table 1
Metal composition of KIGAM Zn–C battery scrap

Fraction	Zn (%)	Mn (%)	Fe (%)
Magnetic	0.02	0.05	10.24
Non-magnetic (+8 mesh)	8.85	2.3	0.12
Non-magnetic (−8 mesh)	15.5	17.5	1.42
Total	24.4	19.8	11.8

have been reported in relation to using hydrogen peroxide in acid media as a reducing agent for manganese dioxide. Under optimum conditions (i.e. pulp density: 50 g L^{-1}, 2 M H_2SO_4, 10 mL H_2O_2, 25 °C, 200 rpm) the maximum dissolution of zinc and manganese were 93.3% and 82.2%, respectively. However, the maximum recovery of 82% Mn did not improve at higher additions of hydrogen peroxide. Sulfuric acid concentrations in excess of 2 M also showed no beneficial effects on both manganese and zinc leaching. Moreover, the leaching of Mn and Zn decreased at higher temperatures (>40 °C) due to the decomposition of hydrogen peroxide at elevated temperatures. The present study investigated the effect of sulfur dioxide as a reducing agent in acid media on the leaching of (i) synthetic material and (ii) KIGAM material at 30 °C. Results are interpreted on the basis of thermodynamic and kinetic aspects and chemical speciation presented in the recent literature on the reductive leaching of oxides [4–8].

2. Experimental

The battery material (503 g) was placed into a set of 11 sieves with mesh widths ranging from 2 mm to 45 μm. These sieves were placed onto a shaker for 2 h and the fractions collected and weighed. Approximately 0.5 g of each size fraction required for analysis was accurately weighed. Aqua regia (20 mL of 1:3 HNO_3:HCl) was added to each sample and digested by gentle boiling on a hot plate for 4 h with the aqua regia being topped up when required. The samples were filtered using sintered glass crucibles and made up to 250 mL. A 100-, 500- or 1250-fold dilution of the liquor was required so that the concentrations were in the working range for the atomic absorption spectrophotometric (AAS) measurement of iron, manganese and zinc, respectively.

Leaching was carried out using a 170 mm × 75 mm (height × diameter) glass reactor. The reactor had four baffles and an impeller with three wings of 6.5 cm diameter. It was operated in a fume hood. All leaching experiments were started at 30 °C with a constant pulp density of 50 g L^{-1}. Other conditions such as sulfuric acid concentration and flow rate were varied. The leach reactor is pictured in Fig. 1.

Sulfur dioxide was introduced into the system either as a blanket or by sparging through the pulp. Blanket introduction of sulfur dioxide occurred when the gas inlet was placed above the liquid; care was taken to flush the reactor vessel of air and allow gas–liquid equilibrium to be established before addition of the battery material.

After each batch of 25 g battery scrap material was introduced to 500 mL of solution a timer was started and 5 mL samples taken using a syringe at relevant time intervals. Each sample was filtered using a clean No. 4 sintered porous crucible, which was reused after being soaked in hydrochloric acid (50%, v/v) overnight and placed in an ultrasonic cleaner for 30 min to remove all solids. The filtrate was made up to 250 mL and a set of dilutions made of this solution. The diluted solutions were analyzed by AAS.

Fig. 1. Glass reactor used in the present study.

Synthetic mixtures were made up using iron(III)–zinc(II)–manganese(IV) oxides. The ratio of these three components matched that of the non-magnetic fraction analyzed by KIGAM. These were sampled and analyzed in the same manner as above.

3. Results and discussions

3.1. Particle size and elemental analysis

Tables 2 and 3 show the particle size distribution and elemental analysis. Particle size ranged from −45 μm to +1.4 mm. The fine fraction contained high Mn (21%) compared to that in coarse fraction (11%); but the Zn and Fe contents in both fractions assayed were approximately the same (20% and ≈3%, respectively). The Mn (21%) and Zn (20%) contents of the fine fraction (−45 μm) of KIGAM material supplied for this work (Table 3) were comparable with the overall values of 20% Mn and 24% Zn reported by the KIGAM researchers (Table 1). The coarse fraction of −1.4 + 1.0 mm contained comparable Zn (20%) and

Table 2
Particle size distribution of KIGAM material used in the present study

Size (μm)	Mass (%)
+2000	0.5
−2000 + 1400	9
−1400 + 1000	10
−1000 + 710	12
−710 + 500	11
−500 + 250	12
−250 + 125	11
−125 + 90	7
−90 + 75	5

Table 3
Elemental analysis of the KIGAM Zn–C scrap material used in the present study

Size (μm)	Zn	Mn	Fe
−1400 + 1000	20	11	3.3
−500 + 250			20
−250 + 125			26
−90 + 45			36
−45	20	21	2.7

Fe (≈3%) but lower Mn (11%). The iron content in the fine fraction was lower (2.7%) compared to the reported overall value (12%).

3.2. Sulfur dioxide leaching of synthetic oxide mixtures

Although sulfur dioxide reacts with water according to Eq. (2), species distribution diagrams [6] show that in acidic (pH < 2) solutions of 0.1 M dissolved sulfur dioxide SO_2 is the predominant species. Thus, the reactions involved in the dissolution of Mn(IV) and Fe(III) oxides are shown by Eqs. (3) and (4), where 's' represents solids while all the others represent dissolved species. The iron(II) sulfate formed in reaction (4) can also be a reducing agent for manganese dioxide as shown in Eq. (5) [7]. Table 4 lists the equilibrium constants for the important chemical reactions. The reductive leaching by H^+/Fe(II) takes place via MnOOH leading to the partial precipitation of iron as the basic sulfate Fe(III)(SO_4)(OH) or oxides Fe_2O_3, Fe_3O_4 or FeOOH due to hydrolysis and/or the increase in Fe(II) concentration in solution especially at elevated temperatures [5]. The relevant reactions are shown by Eqs. (6)–(11).

$$SO_2 + H_2O = H^+ + HSO_3^- \quad (2)$$

$$MnO_2(s) + SO_2 = MnSO_4 \quad (3)$$

Table 4
Equilibrium constants (log K) for reactions of S(IV) and S(VI) species with H^+, Fe^{2+}, Fe^{3+}, Mn^{2+} and Zn^{2+} at 25 °C [9]

Reaction	log K at ionic strength $I = 1$
$H^+ + SO_4^{2-} = HSO_4^-$	1.07 (1.99 at $I = 0$)
$H^+ + HSO_3^- = SO_2 + H_2O$	1.37 (1.77 at $I = 0$)
$H^+ + SO_3^{2-} = HSO_3^-$	6.34 ($I = 1.2$)
$Mn^{2+} + SO_4^{2-} = MnSO_4$	2.26 ($I = 0$)
$Mn^{2+} + SO_3^{2-} = MnSO_3$	3.0 ($I = 0$)
$Fe^{2+} + SO_4^{2-} = FeSO_4$	1.0 (2.3 at $I = 0$)
$Fe^{2+} + SO_3^{2-} = FeSO_3$	1.88
$Fe^{2+} + HSO_3^- = FeHSO_3^+$	1.60
$Fe^{2+} + HSO_4^- = FeHSO_4^+$	0.78
$Fe^{3+} + SO_4^{2-} = FeSO_4^+$	2.23 (4.04 at $I = 0$)
$Fe^{3+} + 2SO_4^{2-} = Fe(SO_4)_2^-$	4.23 (1.34 at $I = 0$)
$Fe^{3+} + HSO_4^- = FeHSO_4^{2+}$	0.78
$Fe^{3+} + SO_3^{2-} = FeSO_3^+$	7.17
$Fe^{3+} + HSO_3^- = FeHSO_3^{2+}$	5.93
$Fe^{3+} + 2H_2O = Fe(OH)_2^+ + 2H^+$	−5.67
$2Fe^{3+} + 2H_2O = Fe_2(OH)_2^{4+} + 2H^+$	−2.72
$Zn^{2+} + SO_4^{2-} = ZnSO_4$	0.89 (2.49 at $I = 0$)
$Zn^{2+} + OH^- = Zn(OH)^+$	4.40 (in $ZnSO_4$ solutions)

Some of these iron(II)/(III) species have been included in E_H-pH diagrams [5–7]; the species distribution diagrams show no evidence for soluble hydroxo-complexes at pH < 3 [12].

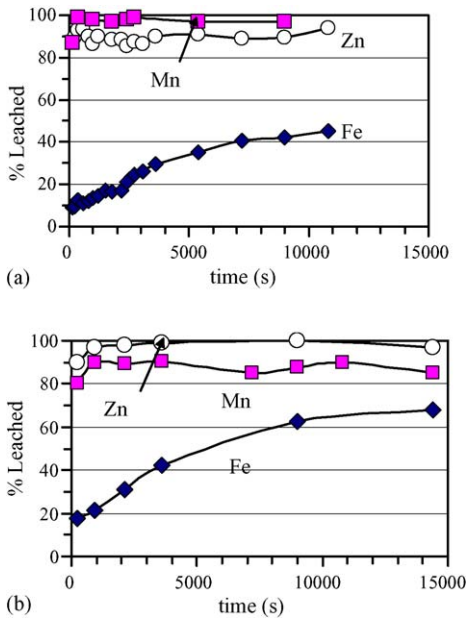

Fig. 2. Metal leaching from a synthetic oxide mixture using different acid concentrations: (a) 2 M H_2SO_4 and (b) 1 M H_2SO_4 (30 °C, 200 mL min^{-1} SO_2 sparge, 25 g L^{-1} pulp density).

$$Fe_2O_3(s) + SO_2 + H_2SO_4 = 2FeSO_4 + H_2O \quad (4)$$

$$MnO_2(s) + 2FeSO_4 + 3H_2SO_4 = MnSO_4 + 2Fe(SO_4)_2^- + 2H^+ + 2H_2O \quad (5)$$

$$MnO_2{\cdot}H_2O(s) + FeSO_4 = MnOOH(s) + Fe(SO_4)(OH)(s) \quad (6)$$

$$MnOOH(s) + 0.5SO_2 + 0.5H_2SO_4 = MnSO_4 + H_2O \quad (7)$$

$$MnOOH(s) + FeSO_4 = MnSO_4 + FeOOH(s) \quad (8)$$

$$Fe(SO_4)(OH)(s) + H_2O = FeOOH(s) + H_2SO_4 \quad (9)$$

$$2Fe(SO_4)(OH)(s) + H_2O = Fe_2O_3(s) + 2H_2SO_4 \quad (10)$$

$$2Fe(SO_4)(OH)(s) + FeSO_4 + 2H_2O = Fe_3O_4(s) + 3H_2SO_4 \quad (11)$$

Fig. 2a and b show the results from the preliminary experiments carried out with synthetic oxide mixtures in solutions of different sulfuric acid concentrations. Both manganese and zinc leached rapidly to give ≈100% and ≈90% dissolution, respectively, in 2 M sulfuric acid in a short time period of 5–10 min (Fig. 2a). The iron dissolution during the same time period was only 10%, indicating selective dissolution. This is in accordance with the faster leaching kinetics of manganese dioxide compared to iron oxide by sulfur dioxide [4–8].

A comparison between Fig. 2a and b shows a high iron dissolution up to 65% at a low acid concentration of 1 M H_2SO_4 (Fig. 2b) compared to 45% dissolution in 2 M H_2SO_4 (Fig. 2a).

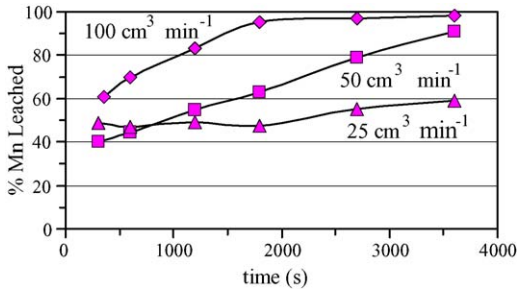

Fig. 3. Leaching of manganese for the fraction −500 + 250 μm at 30 °C, 0.1 M H_2SO_4, 900 rpm with variable blanketed SO_2 flow rates.

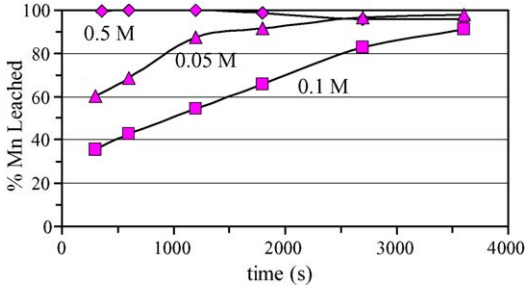

Fig. 4. Leaching of manganese for the fraction −90 + 45 μm at 30 °C, 100 mL min^{-1} blanketed SO_2, 900 rpm with variable acid concentrations.

This detrimental effect of high sulfate represents the possibility of precipitation of iron via Fe(III)(SO_4)(OH) in concentrated acid/sulfate solutions noted in a recent study [5]. The dissolution of zinc is also lower in 2 M H_2SO_4 (≈90%, Fig. 2a) compared to that in 1 M H_2SO_4 (≈100%, Fig. 2b). Again, this shows the possibility of co-precipitation of zinc(II) with iron(III). This is supported by the evidence for the formation of basic complexes such as $(ZnOH)_2SO_4$ [9]. Thus, zinc is seen to have a lower dissolution of 90% at high acid concentration (Fig. 2a) while manganese dissolution is lower at around 90% with a low acid concentration of 1 M (Fig. 2b).

3.3. Sulfur dioxide leaching of KIGAM Zn–C battery scrap

The leaching behavior of manganese in different size fractions was studied using a standard pulp density of 50 g L^{-1}. Results from the experiments are summarized in Figs. 3–7. An increase in sulfur dioxide flow rate increased the rate of manganese dissolution (Fig. 3). Variability of the acid concentration gave some interesting kinetic results. Fig. 4 shows that 0.5 M

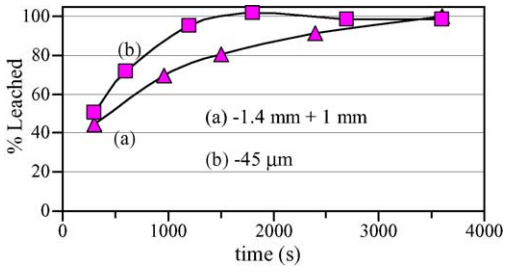

Fig. 5. Effect of particle size on manganese leaching (30 °C, 200 mL min^{-1} blanket SO_2 and 0.1 M H_2SO_4).

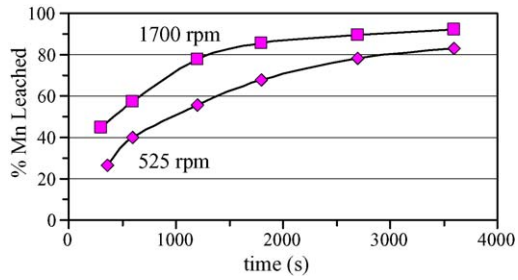

Fig. 6. Effect of agitation speed on manganese dissolution (−250 + 125 μm size fraction, 30 °C, 0.1 M H_2SO_4, 100 mL min^{-1} blanketed SO_2).

H_2SO_4 gave the best initial manganese dissolution rate, but the lowest dissolution rate was found using 0.1 M H_2SO_4, not the 0.05 M H_2SO_4 as expected. This may be due to the formation of Mn(II) and Mn(III) species such as Mn(II)SO_3, Mn(II)SO_4, Mn(II)(OH)HSO_4 and Mn(III)(SO_4)(OH) [5,6] which warrants further studies in this area:

$$MnO_2(s) \cdot H_2O + SO_2 = MnOOH(s) + HSO_3 \quad (12)$$

$$MnOOH(s) + HSO_3 = MnSO_4 + H_2O \quad (13)$$

$$MnOOH(s) + HSO_3 = Mn(II)(OH)HSO_4(s) \quad (14)$$

$$Mn(II)(OH)HSO_4(s) + SO_2 = MnSO_3 + H_2SO_4 \quad (15)$$

$$Mn(II)(OH)HSO_4 = MnSO_4 + H_2O \quad (16)$$

The effect of particle size fits well to what was expected (Fig. 5), where larger particle size led to slower kinetics. Fig. 6 demonstrates that increasing the stirring rate had a positive effect on dissolution of manganese. The effect of different flow rates of SO_2 sparging at a low acid concentration of 0.1 M is shown in the data plotted in Fig. 7a and b. At the lower rate of gas

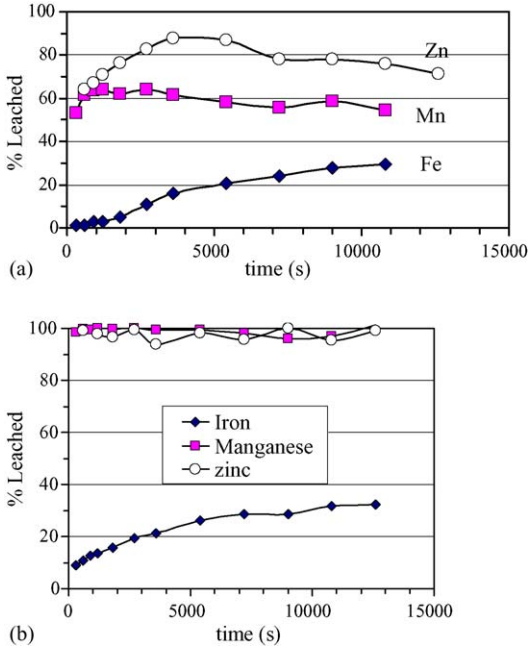

Fig. 7. Metal leaching using different SO_2 sparge rates: (a) 100 mL min^{-1} and (b) 200 mL min^{-1} (−45 μm size fraction at 30 °C, 0.1 M H_2SO_4, 900 rpm).

bubbling, there was a decrease in the concentrations of zinc and manganese extraction at extended reaction times (Fig. 7a). This is consistent with the findings of Rabah et al. [10] and shows re-precipitation of dissolved metal ions which did not occur when a higher flow rate of 200 mL min^{-1} was used. At the higher flow rate all of the manganese and zinc dissolved (Fig. 7b). Further support for the formation of solids on the particle surface can be presented on the basis of kinetic models.

3.4. Kinetic models for iron and manganese leaching

Previous studies showed that the reductive leaching of manganese dioxide and iron oxides follows a shrinking sphere model described by Eq. (17) [4,6,8]. However, the reductive leaching of iron from limonitic nickel laterite and the reductive leaching of manganese from manganiferous ore followed a shrinking core kinetic model described by Eq. (18) [5,7]:

$$1 - (1 - X)^{1/3} = kC\left(\frac{t}{\rho r}\right) = k_{ss}t \quad (17)$$

$$1 - 3(1 - X)^{2/3} + 2(1 - X) = 6DC\left(\frac{t}{\rho r^2}\right) = k_{pl}t \quad (18)$$

where X is the fraction of metal leached after time t (s), C the concentration of reagent which reacts at the surface (mol cm^{-3}), r the initial particle radius of solid (cm), ρ the molar concentration of the dissolving metal ion in the solid (mol cm^{-3}), D the diffusion coefficient ($cm^2\ s^{-1}$), k the intrinsic rate constant of the surface reaction (cm s^{-1}), k_{ss} the apparent rate constant of the shrinking sphere model (s^{-1}) and k_{pl} is the apparent rate constant of the shrinking core model with an insoluble product layer (s^{-1}).

The shrinking sphere model given by Eq. (17) assumes that the solid particle remains as a perfect sphere during the course of reaction. It also assumes that surface reaction is the rate controlling step with an intrinsic rate constant k (cm s^{-1}). The decrease in rate with time is a result of the decrease in particle radius which leads to a decrease in surface area [11]. In contrast, the shrinking core model given by Eq. (18) assumes that the particle radius remains the same because of the build up of a product layer on the surface as the reaction proceeds. Thus, the rate is controlled by the rate of diffusion of reactants from bulk solution to the reaction sites on the surface, or the diffusion of products from the reacting surface to the bulk solution, through the product layer. In this case the decrease in rate with time is assumed to be due to the increase in thickness of the product layer with time [11]. The validity of these models can be tested by plotting $1 - (1 - X)^{1/3}$ or $1 - 3(1 - X)^{2/3} + 2(1 - X)$ against t. These plots should give linear relationships with slopes of k_{ss} (Eq. (17)) or k_{pl} (Eq. (18)) depending on the validity of the kinetic model, where ss represents a shrinking sphere and pl represents a product layer.

Fig. 8 shows the shrinking sphere and core models for the dissolution of iron from synthetic oxide mixture in 1 M and 2 M sulfuric acid solutions based on the results reported in Fig. 2a and b. In both cases the leaching results show a better fit with the shrinking core kinetic model. The apparent rate constants (k_{pl})

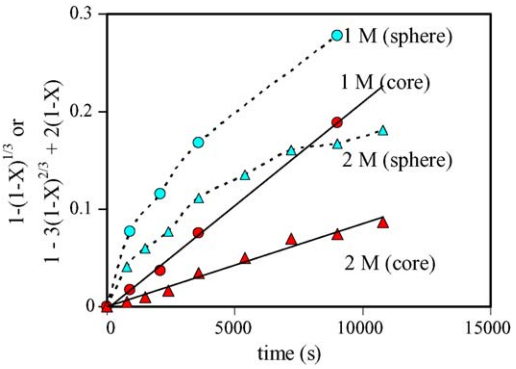

Fig. 8. Shrinking sphere and core models for the dissolution of iron from synthetic Fe(III)–Mn(IV)–Zn(II) mixture (data from Fig. 1a and b).

based on the slopes of linear relationships are $2 \times 10^{-5}\ s^{-1}$ (2 M acid) and $1 \times 10^{-5}\ s^{-1}$ (1 M acid). These values are of the same order as the previous results reported for the reductive leaching of iron from limonitic laterite ore at 90 °C using SO_2/H_2SO_4 [5]. Fig. 9a plots the kinetic models for the dissolution of manganese from the fine fraction based on the results summarized in Fig. 5. The non-linear relationships in both cases may be related to the non-uniform size fraction, because the fine fraction contained a range of sizes <45 μm.

Fig. 9b shows the plots relevant to the two models based on the results for the coarse fraction (−1.4 + 1 mm, Fig. 5) which represents a limited range of particle sizes. It is clear that the shrinking core model shows a better linear relationship. This is also consistent with the shrinking core model demonstrated by the reductive leaching of manganese from a manganiferous ore [7]. Likewise Fig. 10 shows a good linear relationship corresponding to the

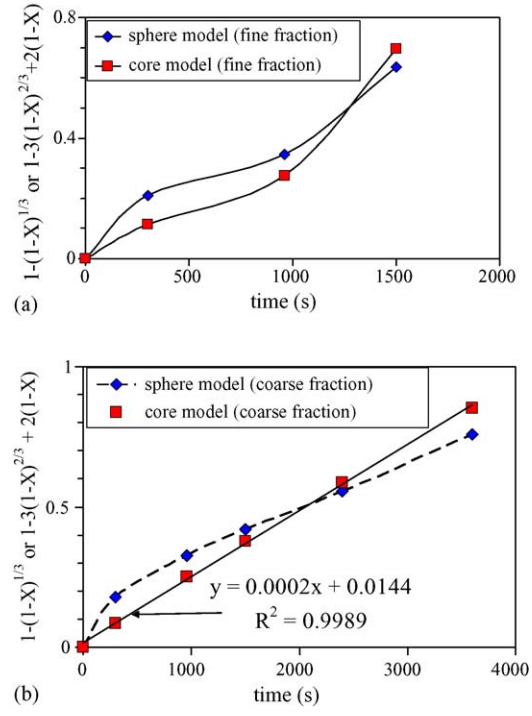

Fig. 9. Shrinking sphere and core models for the dissolution of manganese from (a) fine fraction and (b) coarse fraction (data from Fig. 5).

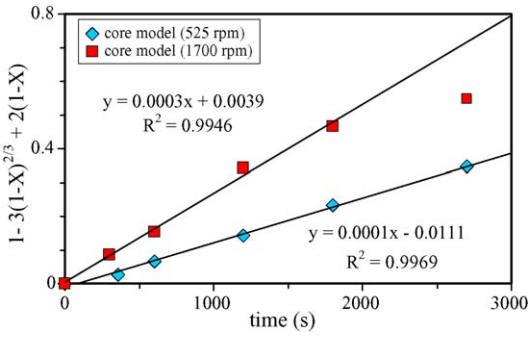

Fig. 10. Shrinking core model for the dissolution of manganese at different rotation speeds (data from Fig. 6).

shrinking core model for the results shown in Fig. 6 for the two experiments carried out at different rotation speeds 525 rpm and 1700 rpm. Thus, it is clear that re-precipitation of some of the dissolved metal ions on the particle surface according to Eqs. (6)–(15) is largely responsible for the decrease in metal ion concentration over the extended periods of leaching times shown in Fig. 7a.

Future work will include the separation and electrolytic recovery of zinc and manganese dioxide, which have been successfully tested by previous researchers [3,13,14].

4. Summary and conclusions

- The preliminary results obtained with synthetic mixtures of Zn(II)–Mn(IV)–Fe(III) oxides of the same composition as the zinc–carbon battery scrap provided by KIGAM show similar trends in leaching of these three metals by SO_2/H_2SO_4 at 30 °C.
- The leaching rates depended upon the sulfur dioxide flow rates, particle size, acid concentration and agitation.
- Both Mn and Zn dissolution with 0.1 M H_2SO_4 at a SO_2 flow rate of 200 mL min^{-1} was nearly 100% with a low Fe dissolution of 10% in 15 min of leaching of the fine fraction (Fig. 7b). The same fraction gave nearly 100% dissolution of Mn in 30 min when 200 mL min^{-1} blanket of SO_2 was used with 0.1 M H_2SO_4 (Fig. 5). Under the same conditions the coarse fraction gave 85% Mn dissolution.
- Thus, the SO_2/H_2SO_4 leaching of KIGAM material offered higher Mn and Zn dissolution at faster rates even at a low temperature (30 °C) and low acid concentration (0.1 M H_2SO_4), compared to the previously reported leaching results with strong alkali or peroxide and strong acid at relatively high temperatures of 40–60 °C.
- Low sulfur dioxide is likely to re-precipitate some of the dissolved metal ions on prolonged leaching. This was confirmed by the fact that the leaching of manganese demonstrates a shrinking core model indicating that the diffusion of reactants or products through an insoluble product layer is the rate controlling step.

Acknowledgements

The authors wish to thank the International Science Linkages Program of the Department of Education, Science and Technology, and the Parker Centre for the provision of funding for RC to undertake this project. The Parker Centre is supported through the Commonwealth Government Cooperative Research Centre's Program. We are also grateful to the Korean Institute of Geoscience and Mineral Resources for the provision of spent battery material for the experimental work and for the interest shown in the project by Dr. Dong-Jin Kim, Dr. Jae-Chun Lee and Dr. Jeong-Soo Sohn.

References

[1] S. Panero, C. Romoli, M. Achilli, E. Cardareli, B. Scrosati, Impact of house hold batteries in landfills, J. Power Sources 57 (1995) 9–12.
[2] L. Pietrelli, I. Gaballah, J. Hager, R. Solozabal, Proceedings of Global Symposium on Recycling, Waste Treatment and Clean Technology, vol. 1, TMS, Warrendale, PA, 1999, pp. 675–680.
[3] A.L. Salgado, A.M.O. Veloso, D.D. Pereira, G.S. Gontijo, A. Salum, M.B. Mansur, Recovery of zinc and manganese from spent alkaline batteries by liquid–liquid extraction with Cyanex 272, J. Power Sources 115 (2003) 267–373.
[4] J.D. Miller, R.-Y. Wan, Reaction kinetics for the leaching of MnO_2 by sulfur dioxide, Hydrometallurgy 10 (1983) 219–242.
[5] G. Senanayake, G.K. Das, A comparative study of leaching kinetics of limonitic laterite and synthetic iron oxides in sulfuric acid containing sulfur dioxide, Hydrometallurgy 72 (2004) 59–72.
[6] G. Senanayake, A mixed surface reaction kinetic model for the reductive leaching of manganese dioxide with acidic sulfur dioxide, Hydrometallurgy 73 (2004) 215–224.
[7] G. Senanayake, The reductive leaching of manganese dioxide: reaction kinetic models and mechanisms, in: Hydrometallurgy, TMS, 2003, pp. 485–498.
[8] G. Senanayake, A surface reaction kinetic model to compare the reductive leaching of iron from goethite, magnetite and limonitic nickel laterite ores by acidic sulfur dioxide, Metall. Mater. Trans. 34B (2003) 735–739.
[9] L.G. Sillen, A.E. Martell, Stability Constants of Metal Complexes, Chemical Society Special Publication No. 17, London, 1964.
[10] M.A. Rabah, M.A. Barakat, Y.Sh. Mahrous, Recovering metal values hydrometallurgically from spent dry battery cells, J. Met. (1999) 41–43.
[11] O. Levenspiel, Chemical Reactions Engineering, Wiley, New York, 1972.
[12] G. Senanayake, D.M. Muir, Speciation and reduction potentials of metal ions in concentrated chloride and sulfate solutions relevant to processing base metal sulphides, Metall. Trans. 19B (1988) 37–45.
[13] C.C.B.M. De Souza, J.A.S. Tenorio, Simultaneous recovery of zinc and manganese dioxide from household alkaline batteries through hydrometallurgical processing, J. Power Sources 136 (2004) 191–196.
[14] J.M.S. Rodrigues, The production of particulate manganese dioxide from electrowinning, in: Proceedings of the International Symposium on Electrometallurgical Plant Practice 20th Annual Hydrometallurgical Meeting, Pergamon Press, Montreal, Que., 1990, pp. 199–220.